Highly Water-Permeable Metal-Organic Framework MOF-303 Membranes for Desalination

Cong, Shenzhen; Yuan, Ye; Wang, Jixiao; Wang, Zhi; Kapteijn, Freek; Liu, Xinlei

DOI
10.1021/jacs.1c10192

Publication date
2021

Document Version
Final published version

Published in
Journal of the American Chemical Society

JACS
JOURNAL OF THE AMERICAN CHEMICAL SOCIETY
pubs.acs.org/JACS
Communication

Highly Water-Permeable Metal–Organic Framework MOF-303 Membranes for Desalination

Shenzhen Cong, Ye Yuan, Jixiao Wang, Zhi Wang, Freek Kapteijn, and Xinlei Liu*

Cite This: *J. Am. Chem. Soc.* 2021, 143, 20055–20058
Read Online

ABSTRACT: New membrane materials with excellent water permeability and high ion rejection are needed. Metal–organic frameworks (MOFs) are promising candidates by virtue of their diversity in chemistry and topology. In this work, continuous aluminum MOF-303 membranes were prepared on α-Al_2O_3 substrates *via* an *in situ* hydrothermal synthesis method. The membranes exhibit satisfying rejection of divalent ions (e.g., 93.5% for $MgCl_2$ and 96.0% for Na_2SO_4) on the basis of a size-sieving and electrostatic-repulsion mechanism and unprecedented permeability (3.0 $L{\cdot}m^{-2}{\cdot}h^{-1}{\cdot}bar^{-1}{\cdot}\mu m$). The water permeability outperforms typical zirconium MOF, zeolite, and commercial polymeric reverse osmosis and nanofiltration membranes. Additionally, the membrane material exhibits good stability and low production costs. These merits recommend MOF-303 as a next-generation membrane material for water softening.

Metal–organic frameworks (MOFs) are a family of porous crystalline materials composed of inorganic metal ions or metal clusters connected by organic ligands *via* coordination bonds.[1−4] Because of their diversity in chemistry and topology, MOFs have been extensively explored for applications such as gas storage, separation, sensing, catalysis, proton conduction, *etc.*[5−7] Significant progresses have been made in fabricating polycrystalline MOF membranes, especially for gas separations.[8−13] However, applications of polycrystalline MOF membranes in water treatment were initially obstructed because of the lack of chemical stability. Although highly water-stable zirconium MOF membranes were unveiled in recent years,[14,15] the related research is still in its infancy. Highly water-permeable MOF membranes with satisfying rejection had been in demand.

Very recently, a water-stable aluminum MOF named MOF-303 (Al(OH)(HPDC); HPDC = 1*H*-pyrazole-3,5-dicarboxylate) was reported.[16−18] It has the *xhh* topology and is constructed from infinite, rodlike $Al(OH)(-COO)_2$ clusters linked through HPDC ligands (Figure S1). In the clusters, octahedrally coordinated Al(III) ions are corner-shared bound by four bridging carboxyl and two hydroxyl groups. MOF-303 features a three-dimensional framework with one-dimensional (1D) rhombic channels (open space of ~0.6 nm) along the *a* axis.[16] The clusters and ligands endow the 1D channels with hydrophilic sites. The high pore volume together with the hydrophilic nature of the framework was translated into impressive water capacity. Besides, fast sorption kinetics was observed and was attributed to the 1D hydrophilic channels, which created a favorable situation for the formation of well-defined water cluster structures.[17,19] Furthermore, the pore opening size of the 1D channels is around 0.60 nm in diameter, which is between the diameters of water molecules (0.28 nm) and common hydrated ions (≥0.66 nm) (Table S1).[20] Therefore, water desalination can be realized through the size-exclusion mechanism (Figure 1). Additionally, cheap metal and ligand sources are available, and water can be used as the solvent for the production of MOF-303. The above merits of MOF-303 satisfy the prerequisites of a high-performance membrane material for water desalination to mitigate the shortage of fresh water. However, to the best of our knowledge, no dense polycrystalline MOF-303 membranes have been unveiled.

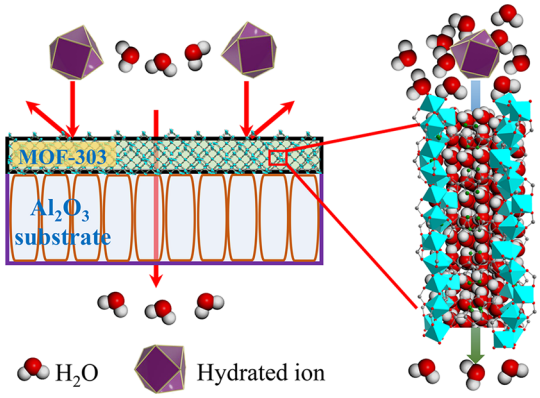

Figure 1. Schematic representation of water desalination with a metal–organic framework MOF-303 membrane.

In this work, to harness these properties inside energy-efficient membranes, continuous polycrystalline MOF-303 membranes supported on porous alumina disks were fabricated *via* an *in situ* hydrothermal synthesis method. The as-

Received: September 26, 2021
Published: November 23, 2021

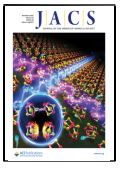

https://doi.org/10.1021/jacs.1c10192
J. Am. Chem. Soc. 2021, 143, 20055–20058

synthesized membranes exhibited high rejection of divalent ions and unprecedented permeability, recommending MOF-303 as an excellent membrane material for water softening.

The stability of MOF-303 powder in saline water was tested before membrane fabrication. MOF-303 powder was suspended in various saline aqueous solutions (0.10 wt % KCl, NaCl, or $MgCl_2$) at 50 °C. The concentration of MOF-303 in these solutions was relatively low (0.04 wt %), and adequate water solutions were used in case the stability was concentration-dependent.[19] After treatment for 50 days, both the crystalline structure and morphology of MOF-303 were well-retained, as evidenced by the X-ray diffraction (XRD) patterns and scanning electron microscopy (SEM) images, respectively (Figures S3 and S4).

Since no recipes for fabricating polycrystalline MOF-303 membranes were disclosed, the amount of metal source, ligand, alkali and solvent, temperature, duration, and the type and roughness of the substrate were thoroughly studied in this work to yield sufficient growth nuclei and form fairly well intergrown membrane structures. Finally, an optimal recipe was obtained (see the Supporting Information for details): the Al^{3+}:H_3PDC:NaOH:H_2O molar ratio was fixed at 1:1:2:2000; the proper temperature and duration were 100 °C and 48 h, respectively; and porous α-Al_2O_3 disks with an asymmetric configuration (70 nm average pore size for the top layer) were preferred as substrates. Porous alumina, which has been widely used in commercial crystalline zeolite membrane modules because of its low transport resistance, easy scale-up, good chemical stability, and fantastic thermal stability,[21] was employed as the substrate. In addition, the surface of the alumina substrate can partially dissolve under alkaline conditions, and the released Al will coordinate with HPDC ligands, facilitating the nucleation and growth of MOF-303 membranes.

As indicated in Figure 2a,b, the surface of the substrate is completely covered with well-intergrown crystals with no visible cracks or pinholes. The crystals have sharp edges with sizes between 1.0 and 4.0 μm, yielding a membrane thickness of around 4.0 μm (Figure S10). The crystalline structure and random packing of the grains were confirmed by the XRD patterns (Figure 2c).

To confirm the integrity of the as-synthesized membrane, single-gas permeation measurements were performed with a soap-film flowmeter at room temperature (25 ± 2 °C) under a transmembrane pressure of 1.0 bar (see the Supporting Information for details). As shown in Figure 3, the H_2 permeance is about 1.2×10^{-6} mol·m^{-2}·s^{-1}·Pa^{-1}, and the ideal selectivities for light-gas pairs (6.3, 3.9, and 2.9 for H_2/CO_2, H_2/N_2, and H_2/CH_4, respectively) are close to the corresponding Knudsen diffusion ratios (4.7, 3.7, and 2.8, respectively). The size-sieving effect is illustrated by the H_2/C_3H_8 and H_2/i-butane pairs, with ideal selectivities of 21.8 and 49.6 and Knudsen diffusion ratios of 4.7 and 5.4, respectively. These results verify that the polycrystalline membrane is continuous, highlighting its integrity.[22] No sharp cutoff between H_2 and other gases was observed, probably because the pore size of MOF-303 (~0.60 nm) is larger than their kinetic diameters (~0.29, 0.33, 0.36, 0.38, 0.42, and 0.50 nm for H_2, CO_2, N_2, CH_4, C_3H_8, and i-butane, respectively).[23] The fluctuation of gas permeance with kinetic diameter can be rationalized in terms of the interplay of adsorption and diffusion effects.

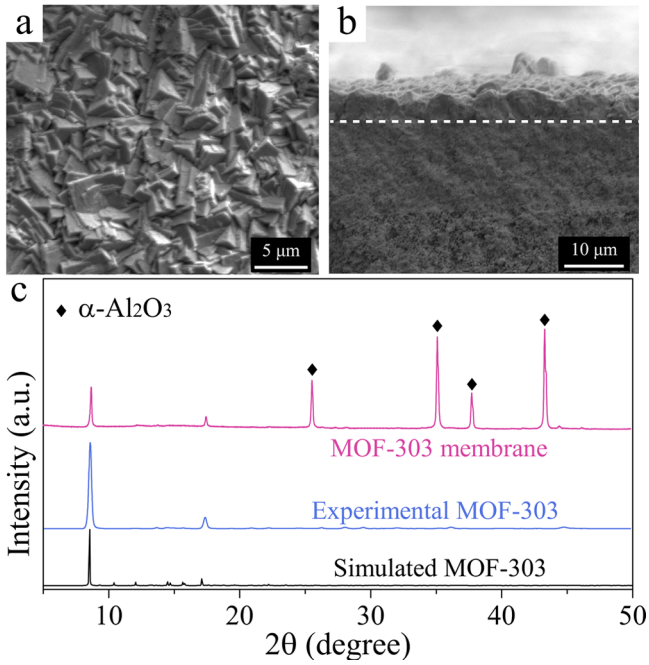

Figure 2. (a) Top view and (b) cross-sectional SEM images of a MOF-303 membrane. The dashed line in (b) distinguishes the membrane layer and substrate. (c) XRD patterns of experimental MOF-303 powder and membrane. The simulated one is provided for comparison.

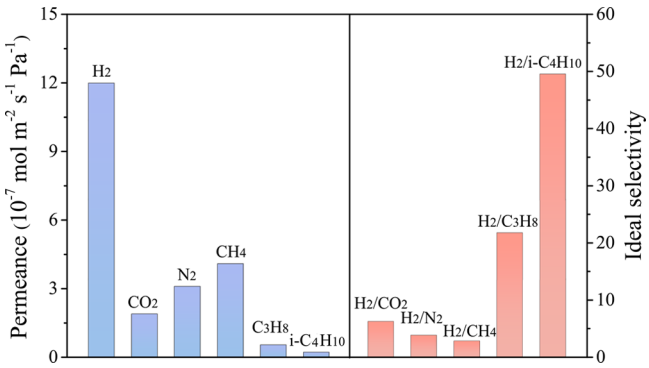

Figure 3. Single-gas permeance and ideal selectivity of a MOF-303 membrane. The operation temperature was 25 ± 2 °C under a pressure difference of 1.0 bar. The pressure of the permeate side was kept under ambient conditions.

The continuous MOF-303 membrane was applied for water desalination. Five different salt solutions (containing KCl, NaCl, $CaCl_2$, $MgCl_2$, or Na_2SO_4) with the same concentration (0.10 wt %) were prepared as feeds. The measurements were carried out in a dead-end system (Figure S6) at room temperature (25 ± 2 °C) with a transmembrane pressure of 5.0 bar. Each salt passed through the membrane in a manner of ion pairs to conserve electroneutrality.[24] The membrane rejection for different salts was determined by testing the ion conductivity in the retentate and permeate with a conductivity meter. The permeance was obtained on the basis of the permeated volume, membrane area, duration of permeate collection, and transmembrane pressure (see the Supporting Information for details).

As depicted in Figure 4a, the membrane rejection roughly increases with hydrated ion diameter (in nm, K^+ (0.66) = Cl^-

https://doi.org/10.1021/jacs.1c10192
J. Am. Chem. Soc. 2021, 143, 20055−20058

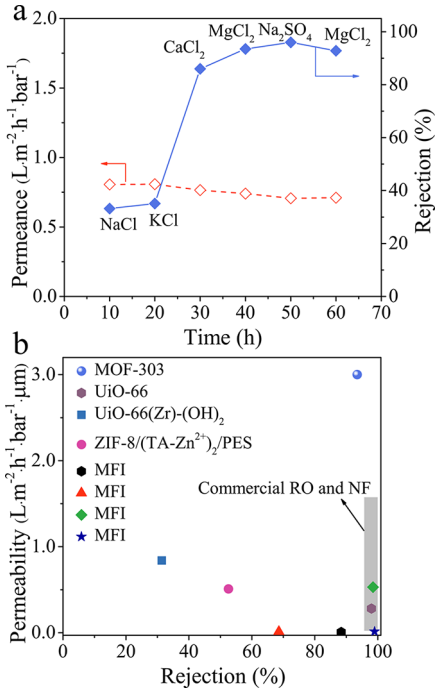

Figure 4. (a) MOF-303 membrane separation performance for water desalination. The feed concentration of each solution (KCl, NaCl, $CaCl_2$, $MgCl_2$, or Na_2SO_4) was 0.10 wt %. The operation temperature and transmembrane pressure were 25 ± 2 °C and 5.0 bar, respectively. The system was flushed with deionized water and dried when the feed was changed. (b) Desalination (Mg^{2+} retention) performances of MOF-303, zeolite, commercial polymeric reverse osmosis (RO) and nanofiltration (NF), and other MOF membranes. Data in Table S2 were used to make the plot in (b).

(0.66) < Na^+ (0.72) < SO_4^{2-} (0.76) < Ca^{2+} (0.82) < Mg^{2+} (0.86)), demonstrating a size-sieving mechanism. The rejection of monovalent ions (33.2% and 35.1% for NaCl and KCl, respectively) is lower than expected. This can be interpreted by the structural flexibility of MOF-303. Although the pore size of MOF-303 is around 0.60 nm as estimated from crystallographic data,[16] an average pore size of 0.80 nm was derived from our Ar adsorption experiment (Figure S5). Hence, good rejection was achieved in the case of divalent ions (93.5% for $MgCl_2$ and 96.0% for Na_2SO_4) when their hydrated ion diameters are close to 0.80 nm. These results further prove the membrane integrity. As rearrangement and dehydration of the water shell surrounding ions could take place during transport,[25,26] reducing their effective size, low concentrations of divalent ions were present in the permeate. Moreover, the flexibility of the MOF-303 framework also accounts for this phenomenon. Although the hydrated ion diameter of SO_4^{2-} is smaller than those of Ca^{2+} and Mg^{2+}, the rejection of Na_2SO_4 is higher than those of $CaCl_2$ and $MgCl_2$. This can be rationalized in terms of the electrostatic-repulsion effect.[27] Carboxyl groups in the ligands of MOF-303 can be ionized, thus endowing the membrane surface with negative charges (Figure S7). The membrane exhibited a moderate permeance (0.74 $L{\cdot}m^{-2}{\cdot}h^{-1}{\cdot}bar^{-1}$). Over the 60 h evaluation, the permeance was well-maintained. Furthermore, constant ion rejection was recognized from repeated tests using $MgCl_2$ solutions (Figure 3a). These results indicate that the crystalline structure and grain boundaries of the membrane, the interfaces between the membrane and substrate, and the substrate were not damaged during the test. Direct evidence can be found from the invariable SEM images (Figure S8) and XRD pattern (Figure S9). Outstanding stability and qualified mechanical strength were proved.

In order to benchmark and compare the intrinsic performance of membrane materials, the membrane thickness was normalized, and the permeability was calculated. As anticipated, the MOF-303 membrane delivers the highest permeability (3.0 $L{\cdot}m^{-2}{\cdot}h^{-1}{\cdot}bar^{-1}{\cdot}\mu m$) combined with satisfying rejection (for Mg^{2+}) (Figure 4b and Table S2). This can be attributed to the high water capacity and fast water sorption kinetics of MOF-303.[17] The hydrophilic 1D channels in MOF-303 could create a favorable situation for the formation of well-defined water cluster structures facilitating water transport.[19] The high water permeability, satisfying rejection for divalent ions, low material cost, and good stability and reproducibility (Table S2) indicate that MOF-303 is a promising next-generation membrane material for water softening. Furthermore, a potential for Li^+/Mg^{2+} separation was demonstrated (Table S3).

In conclusion, continuous polycrystalline MOF-303 membranes were fabricated on porous α-Al_2O_3 substrates *via* an *in situ* hydrothermal synthesis approach. The as-synthesized membranes exhibited high rejection of divalent ions (93.5% for $MgCl_2$ and 96.0% for Na_2SO_4) and unprecedented water permeability (3.0 $L{\cdot}m^{-2}{\cdot}h^{-1}{\cdot}bar^{-1}{\cdot}\mu m$). The high water capacity and fast water sorption kinetics played an important role in this exceptional water permeability. Furthermore, the membranes feature excellent stability and low material cost. These properties indicate that MOF-303 is a promising membrane material for water softening. Since MOF membranes with thickness down to a few tens of nanometers were successfully produced *via* a scalable route,[28] it can be envisaged that after this earliest report there will be some optimal preparation conditions for fabricating supported high-flux MOF-303 membranes with thinner selective layers for practical applications.

■ ASSOCIATED CONTENT

Supporting Information

The Supporting Information is available free of charge at https://pubs.acs.org/doi/10.1021/jacs.1c10192.

Experimental and characterization details, structure of MOF-303, Ar adsorption−desorption isotherms, SEM images and XRD patterns of MOF-303 powders and membranes, zeta potential, and water desalination performance (PDF)

■ AUTHOR INFORMATION

Corresponding Author

Xinlei Liu − *Chemical Engineering Research Center, School of Chemical Engineering and Technology, Tianjin Key Laboratory of Membrane Science and Desalination Technology, State Key Laboratory of Chemical Engineering, Tianjin University, Tianjin 300072, China;* orcid.org/0000-0001-7552-1597; Email: xinlei_liu1@tju.edu.cn

Authors

Shenzhen Cong − *Chemical Engineering Research Center, School of Chemical Engineering and Technology, Tianjin Key Laboratory of Membrane Science and Desalination*

Technology, State Key Laboratory of Chemical Engineering, Tianjin University, Tianjin 300072, China

Ye Yuan − *Chemical Engineering Research Center, School of Chemical Engineering and Technology, Tianjin Key Laboratory of Membrane Science and Desalination Technology, State Key Laboratory of Chemical Engineering, Tianjin University, Tianjin 300072, China*

Jixiao Wang − *Chemical Engineering Research Center, School of Chemical Engineering and Technology, Tianjin Key Laboratory of Membrane Science and Desalination Technology, State Key Laboratory of Chemical Engineering, Tianjin University, Tianjin 300072, China;* orcid.org/0000-0002-5027-2456

Zhi Wang − *Chemical Engineering Research Center, School of Chemical Engineering and Technology, Tianjin Key Laboratory of Membrane Science and Desalination Technology, State Key Laboratory of Chemical Engineering, Tianjin University, Tianjin 300072, China;* orcid.org/0000-0002-8465-687X

Freek Kapteijn − *Catalysis Engineering, Chemical Engineering Department, Delft University of Technology, 2629 HZ Delft, The Netherlands;* orcid.org/0000-0003-0575-7953

Complete contact information is available at: https://pubs.acs.org/10.1021/jacs.1c10192

Notes

The authors declare no competing financial interest.

■ ACKNOWLEDGMENTS

We acknowledge the valuable input from Prof. Y. Zhang at ShanghaiTech University. This work was supported by the National Natural Science Foundation of China (22008171) and the Peiyang Scholars Program (Tianjin University).

■ REFERENCES

(1) Zhou, H.-C.; Long, J. R.; Yaghi, O. M. Introduction to metal−organic frameworks. *Chem. Rev.* **2012**, *112*, 673−674.

(2) Zhou, H.-C.; Kitagawa, S. Metal−organic frameworks (MOFs). *Chem. Soc. Rev.* **2014**, *43*, 5415−5418.

(3) Maurin, G.; Serre, C.; Cooper, A.; Férey, G. The new age of MOFs and of their porous-related solids. *Chem. Soc. Rev.* **2017**, *46*, 3104−3107.

(4) Dincă, M.; Long, J. R. Introduction: porous framework chemistry. *Chem. Rev.* **2020**, *120*, 8037−8038.

(5) Furukawa, H.; Cordova, K. E.; O'Keeffe, M.; Yaghi, O. M. The chemistry and applications of metal-organic frameworks. *Science* **2013**, *341*, 1230444.

(6) Freund, R.; Canossa, S.; Cohen, S. M.; Yan, W.; Deng, H.; Guillerm, V.; Eddaoudi, M.; Madden, D. G.; Fairen-Jimenez, D.; Lyu, H.; Macreadie, L. K.; Ji, Z.; Zhang, Y.; Wang, B.; Haase, F.; Woll, C.; Zaremba, O.; Andreo, J.; Wuttke, S.; Diercks, C. S. 25 years of reticular chemistry. *Angew. Chem., Int. Ed.* **2021**, *60*, 23946−23974.

(7) Freund, R.; Zaremba, O.; Arnauts, G.; Ameloot, R.; Skorupskii, G.; Dinca, M.; Bavykina, A.; Gascon, J.; Ejsmont, A.; Goscianska, J.; Kalmutzki, M.; Lachelt, U.; Ploetz, E.; Diercks, C.; Wuttke, S. The current status of MOF and COF applications. *Angew. Chem., Int. Ed.* **2021**, *60*, 23975−24001.

(8) Ma, X.; Kumar, P.; Mittal, N.; Khlyustova, A.; Daoutidis, P.; Mkhoyan, K. A.; Tsapatsis, M. Zeolitic imidazolate framework membranes made by ligand-induced permselectivation. *Science* **2018**, *361*, 1008−1011.

(9) Peng, Y.; Li, Y.; Ban, Y.; Jin, H.; Jiao, W.; Liu, X.; Yang, W. Metal-organic framework nanosheets as building blocks for molecular sieving membranes. *Science* **2014**, *346*, 1356−1359.

(10) Knebel, A.; Geppert, B.; Volgmann, K.; Kolokolov, D.; Stepanov, A.; Twiefel, J.; Heitjans, P.; Volkmer, D.; Caro, J. Defibrillation of soft porous metal-organic frameworks with electric fields. *Science* **2017**, *358*, 347−351.

(11) Brown, A. J.; Brunelli, N. A.; Eum, K.; Rashidi, F.; Johnson, J.; Koros, W. J.; Jones, C. W.; Nair, S. Interfacial microfluidic processing of metal-organic framework hollow fiber membranes. *Science* **2014**, *345*, 72−75.

(12) Qian, Q.; Asinger, P. A.; Lee, M. J.; Han, G.; Mizrahi Rodriguez, K.; Lin, S.; Benedetti, F. M.; Wu, A. X.; Chi, W. S.; Smith, Z. P. MOF-based membranes for gas separations. *Chem. Rev.* **2020**, *120*, 8161−8266.

(13) Denny, M. S.; Moreton, J. C.; Benz, L.; Cohen, S. M. Metal−organic frameworks for membrane-based separations. *Nat. Rev. Mater.* **2016**, *1* (12), 16078.

(14) Liu, X.; Demir, N. K.; Wu, Z.; Li, K. Highly water-stable zirconium metal-organic framework UiO-66 membranes supported on alumina hollow fibers for desalination. *J. Am. Chem. Soc.* **2015**, *137*, 6999−7002.

(15) Wang, X.; Zhai, L.; Wang, Y.; Li, R.; Gu, X.; Yuan, Y. D.; Qian, Y.; Hu, Z.; Zhao, D. Improving water-treatment performance of zirconium metal-organic framework membranes by postsynthetic defect healing. *ACS Appl. Mater. Interfaces* **2017**, *9*, 37848−37855.

(16) Fathieh, F.; Kalmutzki, M. J.; Kapustin, E. A.; Waller, P. J.; Yang, J.; Yaghi, O. M. Practical water production from desert air. *Sci. Adv.* **2018**, *4*, eaat3198.

(17) Hanikel, N.; Prevot, M. S.; Fathieh, F.; Kapustin, E. A.; Lyu, H.; Wang, H.; Diercks, N. J.; Glover, T. G.; Yaghi, O. M. Rapid cycling and exceptional yield in a metal-organic framework water harvester. *ACS Cent. Sci.* **2019**, *5*, 1699−1706.

(18) Wang, H.; Shi, Z.; Yang, J.; Sun, T.; Rungtaweevoranit, B.; Lyu, H.; Zhang, Y. B.; Yaghi, O. M. Docking of Cu(I) and Ag(I) in metal-organic frameworks for adsorption and separation of xenon. *Angew. Chem., Int. Ed.* **2021**, *60*, 3417−3421.

(19) Liu, X.; Wang, X.; Kapteijn, F. Water and metal-organic frameworks: From interaction toward utilization. *Chem. Rev.* **2020**, *120*, 8303−8377.

(20) Xu, S.; Song, J.; Bi, Q.; Chen, Q.; Zhang, W.-M.; Qian, Z.; Zhang, L.; Xu, S.; Tang, N.; He, T. Extraction of lithium from Chinese salt-lake brines by membranes: Design and practice. *J. Membr. Sci.* **2021**, *635*, 119441.

(21) Rangnekar, N.; Mittal, N.; Elyassi, B.; Caro, J.; Tsapatsis, M. Zeolite membranes−a review and comparison with MOFs. *Chem. Soc. Rev.* **2015**, *44*, 7128−7154.

(22) Lin, Y. S.; Kumakiri, I.; Nair, B.; Alsyouri, H. Microporous inorganic membranes. *Sep. Purif. Methods* **2002**, *31* (2), 229−379.

(23) Breck, D. W. *Zeolite Molecular Sieves: Structure, Chemistry and Use*; John Wiley & Sons: New York, 1974; pp 636−637.

(24) Epsztein, R.; Duchanois, R. M.; Ritt, C. L.; Noy, A.; Elimelech, M. Towards single-species selectivity of membranes with subnanometre pores. *Nat. Nanotechnol.* **2020**, *15*, 426−436.

(25) Lu, C.; Hu, C.; Ritt, C. L.; Hua, X.; Sun, J.; Xia, H.; Liu, Y.; Li, D.-W.; Ma, B.; Elimelech, M.; Qu, J. In situ characterization of dehydration during ion transport in polymeric nanochannels. *J. Am. Chem. Soc.* **2021**, *143*, 14242−14252.

(26) Lu, J.; Zhang, H.; Hou, J.; Li, X.; Hu, X.; Hu, Y.; Easton, C. D.; Li, Q.; Sun, C.; Thornton, A. W.; Hill, M. R.; Zhang, X.; Jiang, G.; Liu, J. Z.; Hill, A. J.; Freeman, B. D.; Jiang, L.; Wang, H. Efficient metal ion sieving in rectifying subnanochannels enabled by metal−organic frameworks. *Nat. Mater.* **2020**, *19*, 767−774.

(27) Childress, A.; Elimelech, M. Relating nanofiltration membrane performance to membrane charge (electrokinetic) characteristics. *Environ. Sci. Technol.* **2000**, *34*, 3710−3716.

(28) Li, W.; Su, P.; Li, Z.; Xu, Z.; Wang, F.; Ou, H.; Zhang, J.; Zhang, G.; Zeng, E. Ultrathin metal−organic framework membrane production by gel−vapour deposition. *Nat. Commun.* **2017**, *8*, 406.